Article: Discoveries

Independent recruitment of different types of phospholipases A2 to the venoms of Caenophidian snakes: the rise of PLA_2-IIE within Pseudoboini (Dipsadidae)

Bayona-Serrano J.D.[1], Grazziotin F.G.[2], Salazar-Valenzuela D.[3], Valente R.H.[4], Nachtigall P.G.[1], Colombini M.[5], Moura da Silva A. M.[5], Junqueira-de-Azevedo I.L.M[1,6*].

1. Laboratório de Toxinologia Aplicada (LETA), Instituto Butantan, São Paulo, Brazil;
2. Laboratório de Coleções Zoológicas (LECZ), Instituto Butantan, São Paulo, Brazil;
3. Centro de Investigación de la Biodiversidad y Cambio Climático (BioCamb) e Ingeniería en Biodiversidad y Recursos Genéticos, Facultad de Ciencias del Medio Ambiente, Universidad Indoamérica, Machala y Sabanilla 170301, Quito, Ecuador;
4. Laboratório de Toxinologia, Instituto Oswaldo Cruz, Rio de Janeiro, Brazil;
5. Laboratório de Imunopatologia, Instituto Butantan, São Paulo, Brazil;
6. Center of Toxins, Immune-Response and Cell Signaling (CeTICS), São Paulo, Brazil

*Corresponding author: Inácio Junqueira de Azevedo

Email: inacio.azevedo@butantan.gov.br

Abstract

Snake venom harbors a wide and diverse array of enzymatic and nonenzymatic toxic components, allowing them to exert myriad effects on their prey. However, they appear to trend toward a few optimal compositional scaffolds, dominated by four major toxin classes: SVMPs, SVSPs, 3FTxs and PLA_2s. Nevertheless, the latter appears to be restricted to vipers and elapids, as it has never been reported as a major venom component in rear-fanged species. Here, by investigating the original transcriptomes from 19 species distributed in eight genera from the Pseudoboini tribe (Dipsadidae: Xenodontinae) and screening among seven additional tribes of Dipsadidae and three additional families of advanced snakes, we discovered that a novel type of venom, PLA_2, resembling a PLA_2-IIE, has been recruited to the venom of some species of the Pseudoboini tribe, where it is a major component. Proteomic and functional analyses of these venoms further indicate that these PLA_2s play a relevant role in the venoms from this tribe. Moreover, we reconstructed the phylogeny of PLA_2s across different snake groups and show that different types of these toxins have been recruited in at least five independent events in caenophidian snakes. Additionally, we present the first compositional profiling of Pseudoboini venoms. Our results demonstrate how relevant phenotypic traits are convergently recruited by different means and from homologous and nonhomologous genes in phylogenetically and ecologically divergent snake groups, possibly optimizing venom composition to overcome diverse adaptative landscapes.

Keywords: phospholipases A_2, protein family evolution, gene co-option, snake venom, Dipsadidae.

Running title: Evolution of the PLA_2 scaffold within rear-fanged snakes.

Introduction

Venomous animals and their toxins have been increasingly scrutinized by researchers from around the world in the last four decades (Fox and Serrano 2007; Fry 2015; Zhang 2015; Mackessy 2021). Studies aiming to understand and alleviate the epidemiological phenomenon of human envenomation by these animals were the main drivers of the toxinological sciences throughout most of human history (Prado-Franceschi and Hyslop 2002a; Otero-Patiño 2009; Junqueira-de-Azevedo et al. 2016; Mackessy 2021; Sevilla-Sánchez et al. 2021). Among the great diversity of vertebrate and invertebrate venomous animals, snakes cause higher proportions of human accidents and deaths worldwide (Prado-Franceschi and Hyslop 2002b; Chippaux 2015; Williams et al. 2019). Therefore, venoms from medically relevant snake species belonging to the Viperidae and Elapidae families, which are characterized by their front-fanged dentitions, are among the better-known animal secretions (Fry 2015; Mackessy 2021). However, most snake diversity lies elsewhere, mainly within the family Dipsadidae (Superfamily: Colubroidea), which contains venom-producing species that have been historically neglected in toxinological studies due to their low medical relevance (Junqueira-de-Azevedo et al. 2016; Uetz et al. 2019; Zaher et al. 2019). These snakes exhibit a diverse array of ecological and morphological traits, which might be mirrored by equally varied venoms (Henderson 1982; de Oliveira et al. 2008; Barbo et al. 2011; Weinstein et al. 2011; Gaiarsa et al. 2013; Giraudo et al. 2014).

Recently, there has been an increased number of works that address venom-related questions for the above-mentioned species that reveal highly complex venom compositions, which resemble the characteristics observed in vipers and elapids.

Moreover, these works have revealed a series of new, poorly characterized venom components that appear to be found only in this group of snakes (de Oliveira et al. 2008; Weinstein et al. 2011; Campos et al. 2016; Junqueira-de-Azevedo et al. 2016; Modahl et al. 2018; Bayona-Serrano et al. 2020; Mackessy 2021). However, there is still a lack any kind of compositional or functional information about the venoms of most dipsadid genera (Junqueira-de-Azevedo et al. 2016; Barua and Mikheyev 2019; Bayona-Serrano et al. 2020). The species addressed thus far have indicated that proteolytic enzymes (e.g., zinc-dependent metalloproteinases), followed by cysteine-rich secretory proteins (CRiSPs) and C-type lectins (CTLs), tend to dominate in their venoms (Ching et al. 2012; Campos et al. 2016; Junqueira-de-Azevedo et al. 2016; Bayona-Serrano et al. 2020). Remarkably, phospholipases A_2 (PLA_2s), a common denominator in the venoms of front-fanged snakes and one of the major effectors of their toxic actions (e.g., myotoxicity, myonecrosis, lipid membrane damage, neurotoxicity, and prey immobilization), have not been assertively associated with venom features in any dipsadid (Junqueira-de-Azevedo et al. 2016; Barua and Mikheyev 2019).

PLA_2s catalyze the hydrolysis of glycerophospholipids at the *sn-2* position, producing free fatty acids and lysophospholipids (Six and Dennis 2000; Huang et al. 2015a). They are ubiquitous in vertebrates, where they fulfill several physiological roles and are divided into three main categories: secretory, cytosolic, and Ca^{2+}-independent PLA_2s, depending on their cellular location and catalytic mechanism (Six and Dennis 2000). Snake venom PLA_2s belong to the secretory type, which has been classically divided into 11 different groups based on their primary structures and the tissues in which they are most commonly expressed (Six and Dennis 2000). Venom PLA_2s have been commonly reported in two front-fanged snake families: the Elapidae family contains

secretory PLA_2s from Group I, and the Viperidae family produces group IIA PLA_2s in their venoms (Ogawa et al. 1995; Jeyaseelan et al. 2000; Huang et al. 2015b; Dowell et al. 2016). These enzymes are generally associated with some of the most severe symptoms observed in accidents involving front-fanged snakes that harbor them as a major toxin class (Gutiérrez et al. 2009; Tsai 2016; Pla et al. 2018; Tasoulis et al. 2020; Mackessy 2021). These enzymes have undergone accelerated evolution and have undergone genetic expansion in front-fanged snakes, where they represent a multigene family with several paralogs (Jeyaseelan et al. 2000; Yamaguchi et al. 2014; Dowell et al. 2016; Suranse et al. 2022).

The contribution of PLA_2s to the venoms of rear-fanged snakes is less evident, and their activity, abundance, structural diversity and evolution might be underestimated (Huang and Mackessy 2004; Fry et al. 2012; Fry 2015; Junqueira-de-Azevedo et al. 2016; Pla et al. 2017; Torres-Bonilla et al. 2018; Mackessy et al. 2020). In 2004, a protein showing PLA_2 catalytic activity and high similarity at its N-terminus to PLA_2-IA from sea snakes was isolated from the venom of the colubrid, *Trimorphodon lambda* (Huang and Mackessy 2004). A few other species were shown to have a different type of PLA_2 in their venoms, PLA_2-IIE, which commonly occurs in the human and mouse brain/heart/uterus and serves physiological functions (Six and Dennis 2000; Suzuki et al. 2000; Mackessy 2021). Transcripts for PLA_2-IIE have been detected at low levels in the venom glands of several snakes, although they never appear to be as preponderant as their I or IIA counterparts found in elapids and vipers, respectively (Fry et al. 2012; Yamaguchi et al. 2014; Pla et al. 2017). *Dispholidus typus* and *Oxyrhopus guibei*, species from two completely different families (e.g., Colubridae and Dipsadidae, respectively), have the highest expression levels of PLA_2-IIE transcripts among rear-fanged snakes

reported thus far (Junqueira-de-Azevedo et al. 2016; Pla et al. 2017). The former is a colubrid that is notorious for its potent venom, being involved in human casualties, including the renowned case of Karl Patterson Schmidt (Pla et al. 2017). On the other hand, *O. guibei*, a dipsadid belonging to the Pseudoboini tribe, is a docile species with a scarce record of human accidents. In 2018, Torres-Bonilla et al. studied the enzymatic actions of the venom of the pseudoboine *Pseudoboa neuwiedii* and found that it had PLA_2 activity levels similar to those observed in viper species. Subsequent proteomic analyses of the venom of *P. neuwiedii* identified peptides belonging to the PLA_2s of group II (Torres-Bonilla et al. 2018). This finding, along with a previous report of PLA_2-IIE transcripts being expressed in the venom gland of *O. guibei*, hinted that PLA_2s might be a relevant venom component in the tribe Pseudoboini.

In this work, we elucidated the occurrence of PLA_2s in the venoms of the Dipsadidae family by scrutinizing the venoms and venom glands of the Pseudoboini tribe and additional outgroups through transcriptomic, proteomic and functional approaches. We reconstructed the evolutionary history of PLA_2-IIE in snakes and discuss the possible recruitment and duplication events that turned this family of proteins into a major player in dozens of rear-fanged species. Moreover, we contrast our findings with previously reported PLA_2s from other snake families and infer that multiple recruitment events have shaped the dispersion of these toxins among caenophidian snakes. Additionally, the data regarding other toxins of the Pseudoboini tribe represent a substantial addition to the poor knowledge of the venom compositions of rear-fanged snakes and bring new research opportunities for the exploration of colubroid venoms.

Results

Venom compositional profile of the Pseudoboini tribe: A PLA_2-IIE-rich group of snakes.

To establish the phylogenetic relationships of species within the Pseudoboini tribe, which is associated with their venom profiles, we used our assembled transcriptomic data to build a dataset of 2161 conserved loci and used them to reconstruct the phylogenetic relationships of the tribe (Supplementary Fig. S1, Supplementary Material online). The full mitochondrial genomes of the individuals were also recovered using the MITGARD approach and used to reconstruct the phylogenetic relationships of the tribe (Supplementary Fig. S2, Supplementary Material online) (Nachtigall, Grazziotin, et al. 2021). Both trees showed similar relationships, but we adopted the tree based on the conserved loci to draw the illustrative tree shown in Figure 1 due to its higher node support values.

Venom gland transcriptome (VGT) annotation of species from this tribe uncovered a wide array of toxin classes, both enzymatic and nonenzymatic, with a varying number of putative paralogs and expression levels (Fig. 1, Supplementary Table S1, Supplementary Material online). Snake venom metalloproteinases from the P-III subtype (SVMP P-III) were a dominant component in all species of the tribe. Despite this protease dominance, we observed great compositional variations, especially regarding CRiSPs and PLA_2s. Based on its toxin expression profiles, the tribe could be divided into two main groups: the *Oxyrhopus-like* group and the *Clelia-like* group (Fig. 1).

[Place for Figure 1]

The *Oxyrhopus-like* group contains species from the genera *Oxyrhopus* and *Siphlophis* that possess VGTs dominated by SVMP-PIII and cysteine-rich secretory proteins (CRiSPs), with lower expressions of C-type lectins (CTL), natriuretic peptides (CNP), snake endogenous matrix metalloproteinases (seMMP-9) and PLA_2-IIE. On the other hand, the *Clelia-like* group contains the genera *Mussurana*, *Phimophis*, *Rhachidelus*, *Pseudoboa*, *Boiruna* and *Clelia*. These genera form a monophyletic group (Supplementary Fig. S1, Supplementary Material online) and showed similar expression levels of minor toxins but an overall higher proportion of PLA_2-IIE, which was the dominant toxin class in some species. Within the *Clelia-like* group, the genera *Pseudoboa*, *Boiruna* and *Clelia* showed the highest expression levels of PLA_2-IIE, and the PCA confirmed that species belonging to these genera cluster closer together and away from other species of the tribe and are more compositionally related (Supplementary Fig. S3, Supplementary Material online).

Most species from the *Oxyrhopus-like* group retained only one PLA_2-IIE transcript, the exception being *O. clathratus*, which retained two PLA_2-IIE transcripts after curation of their VGT (Supplementary Table S1, Supplementary Material online). On the other hand, all species in the *Clelia-like* group possess two different PLA_2-IIE transcripts that show radically different expression levels, one very highly expressed and the other lowly expressed. When looking at the primary amino acid structure of the PLA_2-IIE-derived proteins retained for species of the tribe, we determined that all PLA_2-IIEs from the *Clelia-like* group encoded shorter proteins, which lack a portion of the C-terminal that is present in some of the *Oxyrhopus* group-derived proteins and is the typical structure in endogenous PLA_2-IIEs from other snake groups (Fig. 2A).

[Place for Figure 2]

However, *O. clathratus* had both the long and short forms. Multiple sequence alignments of full-length PLA_2-IIE transcripts revealed that this shorter C-terminus is caused by deletions of 30 bp and 21 bp in Pseudoboini and in the colubrid *Dispholidus typus*, respectively, while all other PLA2-IIEs from the analyzed snakes possess a longer C-terminus (Supplementary Fig. S4, Supplementary Material online). Moreover, when comparing the primary structures from representative sequences of the highly and weakly expressed transcripts from the genera *Pseudoboa*, *Boiruna* and *Clelia* (*Clelia-like* group), we determined that they possess three different heterogeneous portions between them, even though their signal peptides and active sites were similar (Fig. 2B).

Proteomic analyses not only confirmed the occurrence of PLA_2-IIE in the venoms of *P. nigra*, *B. sertaneja* and *C. equatoriana* but also indicated that it was a major constituent of these venoms (Fig. 2B, Supplementary Fig. S5, Supplementary Material Online). Moreover, the predicted protein from the highly expressed transcript in the venom glands was detected in all three species, harboring a higher proportion of mass spectra than the protein from the weakly expressed transcript, even when both were identified as occurring in *B. sertaneja* (Supplementary Table S2, Supplementary Material online). In *C. clelia* and *P. nigra*, only the highly expressed form was detected in the proteome. Other major venom components reported in the VGTs of the tribe, such as SVMPs, CRiSPs and seMMP-9, were also confirmed to be present in the venom of these three species (Fig. 3, Supplementary Table S2, Supplementary Material Online). Moreover, the abundances of identified venom toxins estimated in Scaffold 5 followed the

same compositional trends that we observed in venom gland transcriptomes, with SVMPs and PLA_2-IIE being dominant toxins in *C. equatoriana* and *B. sertaneja* (Supplementary Fig. S5, Supplementary Material Online).

The 3D structures of a highly expressed PLA_2-IIE from *P. nigra*, used as a representative from the *Clelia-like* group; the longer PLA_2-IIE from *O. guibei*, a PLA_2-IIE from *D. typus*; a PLA_2-IIE from *Crotalus adamanteus* and a noncatalytic PLA_2-IIA from *Bothrops jararaca* were predicted with RoseTTAFold (Hiranuma et al. 2021). Comparisons between these structures and the 3D crystal structure of a catalytically active PLA_2-IIA from *B. jararacussu* revealed that some of the shorter PLA_2-IIE forms obtained from the *Clelia-like* group have better RMSD scores across all aligned pairs than the PLA_2-IIE forms obtained from other viper species (Fig. 3).

[Place for Figure 3]

PLA_2-IIEs inside and outside of the Pseudoboini tribe.

The elevated expression levels of PLA_2-IIE found within the Pseudoboini tribe led us to wonder if these were a unique characteristic of this group within dipsadids or if PLA_2s were also dominant in other tribes. We gathered previously generated snake venom transcriptomic data for representative species of seven additional tribes of Dipsadidae and for the available species of Colubridae, Elapidae and Viperidae and screened for PLA_2-IIE-like sequences, as we performed in a previous work (Bayona-Serrano et al. 2020). The analysis indicated that the elevated expression levels of PLA_2-IIE in venom glands

are likely exclusive to the Pseudoboini tribe within Dipsadidae (Supplementary Fig. S6), suggesting that, when present in other groups, the PLA_2-IIE transcript may correspond to the endophysiological protein. A phylogenetic tree reconstruction performed using PLA_2 sequences from elapids, vipers, colubroids and other vertebrates revealed that the PLA_2s recovered from Pseudoboini species are nested within the type IIE of PLA_2s from other vertebrates. PLA_2-IIE is the sister group of PLA_2-IIA found on viper venoms (Fig. 4 and Supplementary Figs. S7, S8, S9 and S10, Supplementary Material online). Moreover, PLA_2-IIEs recovered from the *Oxyrhopus* group separate themselves from those of the *Clelia-like* group. Interestingly, within the *Clelia-like* group, the highly and weakly expressed transcripts formed separate independent groups. An orthology analysis performed with OrthoFinder clustered all assembled PLA_2-IIEs from Pseudoboini within a single orthogroup, which was probably due to their overall sequence similarity.

Enzymatic assays

Some Pseudoboini venoms tested for PLA_2 activity showed activities comparable to those of viper venoms (Fig. 5). Comparisons were made among four different groups: venoms from viper species known to possess PLA_2 activity, venoms from dipsadids shown to be devoid of PLA_2s, species from the *Oxyrhopus* group and species from the *Clelia-like* group. We observed significant differences between the PLA_2 activities found in species from the *Clelia-like* group and species from the *Oxyrhopus* group. The latter were statistically equal to venom from other dipsadids. For the comparison between activity levels from viper venoms and venoms from the *Clelia-like* group, we were unable to find statistically significant differences, although crude venoms from *C. Clelia* and *B.*

sertaneja presented higher enzymatic activity values than the crude venom of *B. jararacussu*, which is known to be one of the most PLA_2-rich species of snake (Freitas-De-sousa et al. 2020) (Fig. 5).

[Place for Figure 5]

Discussion

The phylogenetic analyses allowed us to reconstruct a robust topology for the sampled species of the Pseudoboini tribe and take advantage of the multigene approach that high throughput transcriptomics generate. Our results allowed us to resolve some internal relationships within the tribe, which clustered the genus *Rhachidelus* along with the monophyletic group formed by *Pseudoboa*, *Clelia* and *Boiruna* (Zaher et al. 2019) (Supplementary Figs. S1 and S2).

The venoms from the Pseudoboini tribe showed the same protease-rich profiles observed in most dipsadids (Junqueira-de-Azevedo et al. 2016; Bayona-Serrano et al. 2020). SVMPs remain a major toxin class in the venoms of these snakes, and elevated levels of CTLs, CRiSPs and seMMP-9 point to them as the usual players in Dipsadidae venoms. However, we noticed unusually high proportions of PLA_2s in this tribe, both in their VGTs and proteomes. The PLA_2s amounts were particularly high in the *Clelia-like* group, in which the PLA_2-IIE expression levels ranged from ~1% to ~27% of whole transcriptomes (Fig. 1, Supplementary Table S1). These high expression levels were found to be exclusive to the Pseudoboini tribe, at least among the species sampled in our screening (Supplementary Fig. S6). All other analyzed tribes within the family had TPM values near zero for PLA_2-like contigs. Regarding other snake families (e.g., Colubridae,

Elapidae and Viperidae) that were screened, we also found almost null expressions of PLA_2-IIE-like contigs. However, previous works have reported PLA_2s from both type IA and IIE as venom components in some species of the Colubridae family (Huang and Mackessy 2004; Fry et al. 2012; Pla et al. 2017; Mackessy et al. 2020). This indicates that there might be other PLA_2s hidden in specific snake groups. An in-depth sampling of venom-producing colubroids is needed to truly determine their occurrence across all advanced snake clades.

Functional analyses of Pseudoboini venoms revealed high PLA_2 activities, which were comparable to those of viper venoms, in species from the *Clelia-like* group (Fig. 5). These findings, along with the fact that highly expressed PLA_2-IIE was found in the analyzed venom proteomes of the group, suggest that this form is responsible for the catalytic PLA_2 activity observed. Previous works had already reported high PLA_2 activity in the venom of *Pseudoboa neuwiedii* (Torres-Bonilla et al. 2017; Torres-Bonilla et al. 2018). However, proteomic analyses of the venom of that species identified an ~14-15 kDa SDS–PAGE band as PLA_2-IIA. In that work, the identified spectra were searched against the UniProtKB/Swiss-Prot database, which found several peptides that matched a myotoxic noncatalytic PLA_2-IIA from *Bothrops moojeni*. However, all PLA_2 we recovered for the tribe, including *P. neuwiedii*, were catalytically active and belonged to the IIE subgroup of PLA_2s. Therefore, we attribute the previous identification of PLA_2-IIA in the venom of *P. neuwiedii* to the general sequence similarity between PLA_2-IIA and PLA_2-IIE and to the lack of representative PLA_2-IIE from Pseudoboini in the databases used in that work (Yamaguchi et al. 2014), which hindered the correct identification of the PLA_2 subtype. It is worth highlighting the considerable PLA_2 activity that we measured for *P. guerini*, since this species had the lowest proportion of PLA_2-IIE

in its VGT within the *Clelia-like* group (Fig. 1). Increased sampling within the genus is needed to confirm whether a highly expressed PLA_2-IIE transcript occurs within its VGTs or if the PLA_2 activity observed is mediated by other means. Species from the *Oxyrhopus-like* group showed no significant differences from the venoms obtained from dipsadids known to be devoid of PLA_2s, in agreement with the low PLA_2-IIE expressions we found in their transcriptomes.

PLA_2 enzymes have been predominantly reported as venom components of front-fanged snakes from the Viperidae family, harboring PLA_2-IIA, and the Elapidae family, harboring PLA_2-IA and PLA_2-IB (Jeyaseelan et al. 2000; Dowell et al. 2016). Interestingly, the genetic organization of the PLA_2-II locus in vipers and other vertebrates suggests that PLA_2s from group IID, which is the evolutionary precursor of all PLA_2-IIA from vipers, was derived from an ancestral duplication of the PLA_2-IIE gene followed by sequential gene duplication and diversification within Viperidae, originating venom PLA_2-IIA toxins (Yamaguchi et al. 2014; Dowell et al. 2016; Koludarov et al. 2019; Suranse et al. 2022). Moreover, genomic data have revealed the presence of exonic debris from the PLA_2-IIE gene spread downstream from the PLA_2-IIE gene in vipers, indicating plausible duplication and pseudogenization events (Dowell et al. 2016; Koludarov et al. 2019). To determine whether these duplications occurred before the diversification of vipers, we analyzed the available genomes of the colubrids *Thamnophis sirtalis* (NCBI accession number NW_013659820.1) and *Pantherophis guttatus* (NCBI accession number NW_023010753.1). We did not find exonic debris for the PLA_2-IIE gene in those species, indicating that the possible duplication of the PLA_2-IIE gene took place after viper diversification and that it does not represent a basal trait in advanced snakes. Therefore, the finding of two types of PLA_2-IIE transcripts showing structural and

quantitative differences in some Pseudoboini species reinforces the hypothesis that the PLA_2-IIE gene has undergone at least one duplication event within the tribe.

Gene duplication is a known trigger of accelerated evolution (Ohno 1971; True and Carroll 2002) that is observed in many venom proteins (Ogawa et al. 1995; Ogawa et al. 2005; Kini and Doley 2010; Vonk et al. 2013; Dowell et al. 2016; Lomonte et al. 2016; Tadokoro et al. 2020). The two types of PLA_2-IIE found in Pseudoboini differ not only in their sequence substitutions but also in the small deletions on their C-terminal portions (Fig. 2A). Previous works have noted that even though the primary structures of IIA and IIE PLA_2s are similar, the C-terminal tails are distinct between them, with PLA_2-IIE having a longer C-terminus (Yamaguchi et al. 2014). Interestingly, a shorter C-terminal deletion was also present in the PLA_2-IIE contig reported for the colubrid *D. typus*, which has moderate levels of PLA_2 expression in its venom glands (~2.75% of whole transcriptome) (Pla et al. 2017). The C-terminal deletion, which shortens the primary structure of the PLA_2-IIE protein, observed only in *D. typus* and in all species from the *Clelia-like* group, constitutes a convergent event in rear-fanged snake groups displaying increased expression levels of this protein type in their venom glands. The role and relevance of this deletion is still not fully understood, but it might indicate a trend toward a more compact IIA-like structural scaffold. The 3D alignments favor this trend, as the PLA_2-IIE from the *Clelia-like* group with a shortened C-terminus showed better alignment scores toward the structure of a viper PLA_2-IIA than the PLA_2-IIEs from other vipers, which do not possess the C-terminal deletion (Fig. 2A and Fig. 3). However, as these 3D alignments were made with predicted structures and the Armstrong error estimate of the models, calculated by RoseTTAFold, always increased toward the C-

terminal portion, it is hard to assertively link this deletion to a trend toward a more IIA-like structure.

The phylogenetic reconstruction of PLA_2 showed that PLA_2-IIEs from Pseudoboini form a sister clade to PLA_2-IIAs from vipers. Within the Pseudoboini tribe, the weakly expressed PLA_2-IIE from *O. occipitalis* possessing the longer C-terminal was the most basal protein, resembling the PLA_2-IIE scaffold found outside of the tribe. Within the *Clelia-like* group, PLA_2-IIE is organized into two separate clades, one containing the highly expressed transcripts and the other containing the weakly expressed transcripts, both harboring the C-terminal deletion (Fig. 4). The highly expressed form was found more consistently in the venom proteome of the genera, with more spectral counts, indicating a higher relative abundance of the protein. We also found that the two clades of sequences had three heterogeneous portions on their primary structures. The implications of these differences are not clear, but it would be expected that the different residues of the highly expressed form contribute to the overall enzymatic efficiency of the protein in the venom.

Outside Pseudoboini, PLA_2-IIE sequences can be retrieved from many snake taxa, mostly from genome annotations or PCR products amplified from various tissues, including the venom glands (Fry et al. 2012; Yamaguchi et al. 2014). There is no strong evidence, however, of PLA_2-IIE being a relevant venom component in other snake families, with the sole exception of the colubrid, *D. typus* (Pla et al. 2017). In this case, combined transcriptomic and proteomic analyses identified PLA_2-IIE among the top three most abundant toxins in the venom. On the other hand, our phylogenetic analysis indicated that the peculiar PLA_2 proteins reported in the colubrid genus, *Trimorphodon*,

are not PLA_2-IIE but belong to the PLA_2-I type, as had been previously reported (Fry et al. 2008) (Fig. 4). The evolutionary history of the PLA_2 gene family in rear-fanged snakes appears to be rather complex, as some species possess PLA_2-IA-like proteins (e.g., *T. lambda*), while others exhibit PLA_2-IIE-like proteins (e.g., *D. typus* and most Pseudoboini species) (Pla et al. 2017; Mackessy et al. 2020).

The genetic scaffold of the PLA_2-II gene cluster is highly conserved in humans, mice, birds and snakes (Huang et al. 2015b). The triplet organization of the locus, with the OTUD3 gene, followed by the PLA_2-IIE gene and then the PLA_2-IID cluster, is mostly maintained in these groups (Huang et al. 2015a; Dowell et al. 2016; Suranse et al. 2022). A PLA_2-IID gene is assumed to be ancestrally recruited in vipers and co-opted into a venom protein, resulting in the modern PLA_2-IIA observed in viper venoms (Yamaguchi et al. 2014; Dowell et al. 2016; Koludarov et al. 2019). This recruitment was followed by sequential gene duplication and accelerated evolution, marked by diverse substitutions at the catalytic site, ultimately generating a noncatalytic (K49) form in some vipers (Huang et al. 2015a; Dowell et al. 2016; Suranse et al. 2022). However, this genetic expansion of the PLA_2-IID cluster, derived from the PLA_2-IIA venom forms found in vipers, has not yet been observed in any other group of advanced snakes. On the other hand, less information is known regarding the genetic scaffolding and evolutionary history of PLA_2-I from elapids. These PLA_2s are structurally divided into group IB, commonly found in mammalian pancreases but also reported in the venoms of some elapid snakes (Armugam et al. 2004; Mackessy 2021), and group IA, which is found almost exclusively in elapid venoms and lacking the "pancreatic loop" characteristic of group IB (Jeyaseelan et al. 2000; Huang and Mackessy 2004; Mackessy 2021). PLA_2-I are placed in a different genomic locus, and their phylogenetic reconstruction indicates that their diversification

was genus-specific and influenced by the ecology and evolutionary history of each lineage (Jeyaseelan et al. 2000). Genomic data from rear-fanged species expressing PLA_2s in their venom are needed to reveal the genomic organization of the PLA_2-I and PLA_2-II gene loci and determine if they are in fact undergoing similar genetic processes as the ones observed in vipers and elapids.

Based on our findings and previous literature reports, we can hypothesize at least three distinct events of recruitment and restriction of PLA_2-like toxins into the venom glands of rear-fanged snakes (Fig. 6). PLA_2s from Group I, which are commonly found in elapid venoms, are apparently recruited to the venom glands of the genus *Trimorphodon*, which has been shown to possess PLA_2-IA-like proteins in its VGTs and proteomes (Huang and Mackessy 2004; Mackessy et al. 2020). This is the first and only record of a non-elapid snake genus harboring PLA_2-I as a venom protein and might indicate that a duplication of the endogenous PLA_2-IB gene, followed by sequential mutations toward an IA-like structure, occurred exclusively in this genus within Colubridae. On the other hand, PLA_2s from group II appear to have been recruited into the venom glands of two separate families of rear-fanged snakes. These enzymes are arranged in a well-characterized cluster that is conserved in various vertebrate lineages and are known to be dominant toxins in vipers, where the PLA_2-IIA gene, evolutionarily derived from PLA_2-IID, has undergone several duplication/loss events. However, a different type of PLA_2-II, PLA_2-IIE, was recruited to the venom arsenal of some species of rear-fanged snakes within the Pseudoboini tribe (Dipsadidae) and the genus *Dispholidus* (Fry et al. 2012; Junqueira-de-Azevedo et al. 2016; Pla et al. 2017). We hypothesize that the PLA_2-IIE gene suffered at least one event of duplication and shortening of the C-terminal tail after Pseudoboini diversification from other Dipsadidae, and this gene was recruited to the venom gland

during the radiation of the *Clelia-like* group. A parallel recruitment of the PLA_2-IIE gene occurred in Colubridae, specifically in the genus *Dispholidus*. The order in which these events took place and whether or not they occurred similarly or simultaneously in both groups is still a matter of investigation.

Moreover, these independent recruitments of PLA_2-IIE and structural changes parallel the better-known evolutionary trajectories of group PLA_2-I in Elapidae and group PLA_2-IIA in Viperidae. Examples of independent recruitment of similar genes to become toxins in different snake groups are now becoming frequent and seem to indicate a trend toward the selection of a few optimal scaffolds to exert toxic functions in snake venom (Campos et al. 2016; Barua and Mikheyev 2019; Bayona-Serrano et al. 2020). The recruitment of PLA_2-IIE to the venom glands of Pseudoboini represents a prime example of this trend.

In summary, although PLA_2s are widespread venom components of several venomous snakes, we suggest that PLA2 became part of the venoms of Caenophidian snakes on at least five occasions and their appearance are not likely to be a basal trait selected early upon the divergence of the group. The PLA_2-IIE gene was recruited and restricted to venoms of the rear-fanged families Colubridae (at least on *D. typus*) and Dipsadidae (Pseudoboini tribe) in two independent events, mirroring the recruitment and expansion of the PLA_2-IIA gene in the Viperidae family (a third event). The PLA_2-I gene, on the other hand, was apparently selected independently in both in Elapidae (fourth event) and in *Trimorphodon*, a specific Colubridae genus (fifth event). Since PLA_2s are associated with some of the major toxic phenotypes of snake venoms, causing a wide array of effects, including cytotoxicity, myotoxicity, neurotoxicity, and many others, it is not surprising that these proteins have been selected multiple times during snake

evolution. Nevertheless, the reiterated recruitment of non-venom PLA_2 genes in different snake families indicates that the intrinsic features of the PLA_2 scaffold make it a valuable asset to effectively impose toxicity in different ecological contexts. Increased genomic sampling of rear-fanged snakes, along with increased functional and structural information from colubroid PLA_2s, is still needed to shed light upon the complex evolutionary history of these toxins within snakes.

[Place for Figure 6]

Materials and Methods

Collection and storage of samples

Specimens from eight genera and 19 species (IBAMA authorization 57585-1 and MAATE authorization MAE-DNB-CM-2019-0115) were collected during a series of field trips to different localities in Brazil and Ecuador. Venom samples were extracted using pilocarpin on sedated individuals as described in previous works (Mackessy et al. 2006). Four days after extraction, the venom glands and other tissues were surgically collected and stored in RNAlater® at -80°C.

RNA extraction and analysis

Tissues were pulverized in a Precellys® 24 homogenizer, and RNA was extracted with TRIZOL® (Invitrogen) following the modification of the method described by Chomczynski and Sacchi (1987) based on the use of guanidine isothiocyanate followed by phenolic extraction (Chomzynski 1987). Total RNA was quantified by Quant-iTTM RiboGreen® RNA reagent and kit (Invitrogen, Life Technologies Corp.). Quality control of the extracted RNA was then performed in an Agilent 2100 Bioanalyzer using an Agilent RNA 6000 Nano kit to verify the integrity of total RNA through band discrimination corresponding to fractions 18S and 28S of total RNA. All procedures involving RNA were performed with RNase-free tubes and filter tips and using water treated with diethylpyrocarbonate (DEPC, Sigma). The general RNA Integrity Number (RIN) obtained for analyzed samples is available in Supplementary Figure S11, Supplementary Material Online.

cDNA library construction and sequencing

Libraries were prepared for each individual sample. One microgram of total RNA was used with an Illumina TruSeq Stranded RNA HT kit consisting of TruSeq Stranded RNA HT/cDNA Synthesis PCR, TruSeq Stranded RNA HT/Adapter Plate Box and TruSeq Stranded HT mRNA. Fragment size distributions were evaluated by microfluidic gel electrophoresis in a Bioanalyzer device (Agilent 2100) using a Agilent DNA 1000 kit according to the manufacturer's protocol. Quantification of each library was then performed by real-time PCR using a KAPA SYBR FAST Universal qPCR kit, according to the manufacturer's protocol, using the StepOnePlusTM Real-Time PCR System. Aliquots of each cDNA library were diluted to a concentration of 2 nM. Next, a pool of all samples, 5 μL of each library, was prepared, and the concentration of the pool was

again determined by real-time PCR. The cDNA libraries were sequenced on an Illumina HiSeq 1500 System in Rapid Run mode using a paired-end flow cell for 300 cycles of 2*151 bp.

Transcriptome assembly and annotation

To assemble the venom transcriptomes of the samples, we checked and removed cross-contamination using an in-house script (Hofmann et al. 2018) that compares sequences from other libraries within the sequencing pool and then trimmed the sequencing adaptors using TrimGalore (Krueger 2015). We merged our reads using PEAR software (Zhang et al. 2014) by taking advantage of the common overlap on the 3` ends that characterizes paired-end short reads (Rokyta et al. 2012) and used those longer merged reads as an input for our assembly. We ran all the assemblies in a standardized way using five different assemblers with different k-mer values and assembly parameters (Trinity: k-mer 31; rnaSPADES: k-mer 31, 75 and 127; Extender: default, overlap 150, and seed size 2000; SeqMan Ngen: k-mer 21; and Bridger: k-mer 30) (Grabherr et al. 2011; Rokyta et al. 2012; Chang et al. 2015; Holding et al. 2018; Bushmanova et al. 2019). Then, we performed toxin annotation using ToxCodan (Nachtigall, Rautsaw, et al. 2021) against a curated dataset of toxin sequences. Annotated toxin transcripts were manually reviewed and used to purge toxic-like contigs from the Trinity assembly of each individual. Then, both annotated toxin sequences and the remaining nontoxin Trinity contigs were combined to obtain a complete venom gland transcriptome of each individual, in which the toxin transcripts were curated. The coding sequences from nontoxin-purged contigs were predicted using CodAn with the full vertebrate model (Nachtigall, Kashiwabara, et al. 2021) and annotated by Blast searches against NCBI nr

and PFAM following the ToxCodan pipeline available online (Nachtigall, Rautsaw, et al. 2021). The expression levels of each individual transcript were estimated using RSEM software (Li and Dewey 2011) after mapping the merged reads from each sample using Bowtie2 and were measured in transcripts per million (TPM) (Bankar et al. 2015).

Proteomic analyses

Analyses by reversed-phased nano chromatography coupled to tandem mass spectrometry analyses of the venoms from three species were performed by the Florida State University College of Medicine Translational laboratory and by the Laboratory of Toxinology (FIOCRUZ, Rio de Janeiro), as detailed in the supplementary methods, Supplementary Material online. Protein identifications of the obtained spectra were performed using MASCOT (Matrix Science, London, UK; version 2.6.2) and X! Tandem (The GPM, thegpm.org, last accessed August 3, 2020; version X! Tandem Alanine [2017.2.1.4]) as the search engine. We considered a 99% and 95% threshold for protein and peptide identification, respectively. Custom-generated FASTA databases containing curated sequences of identified toxins for each specimen and translated protein sequences from the assembled transcriptome (Trinity contigs) for the species were used as a database for spectral identification, as detailed in the supplementary methods, Supplementary Material online. To quantify the estimated abundance of each toxin class, we normalized the total spectra of all identified proteins using the Normalized Spectral Abundance Factor (NSAF) as implemented in Scaffold 5 (Zybailov et al. 2006).

Venom variation and complexity within the tribe

We transformed the expression data using the log-rate (clr, center log-ratio) transformation method (Egozcue et al. 2003; Filzmoser et al. 2009) and applied the functions implemented in the *robCompositions* package (Templ et al. 2011) in the R environment. We used the *clr* transformation for visualization purposes, as it takes the simplex data into real space while retaining the individual identities of each toxin class. With these transformed values, we performed a principal component analysis (PCA) to evaluate the toxin compositions of the sampled Pseudoboini species. We used the *prcomp* function from the stats package in R version 4.1.0 (Team 2015). Then, we separated the poorly represented toxins (i.e., with average expressions of less than 1% of the total toxins) and grouped them into a category called "OtherToxins", which was compared with the main toxins of the tribe. The graph was plotted using the *ggplot* package (Wickham 2016), and different colors were assigned for each analyzed species.

Phylogenetic and evolutionary analyses of PLA_2s in snakes

We screened for PLA_2-IIE-like contigs among four different snake families and seven additional tribes within Dipsadidae using an approach similar to that of Bayona-Serrano et al. 2020 (Bayona-Serrano et al. 2020). Briefly, we performed BlastN searches using *de novo* assembled contigs from Trinity against the curated database of PLA_2-IIE-like sequences obtained herein. The expression of each individual contig was calculated using RSEM (Li and Dewey 2011) by mapping the reads from each sample using Bowtie2. Expressions were estimated in transcripts per million (TPM) (Wagner et al. 2012; Wagner et al. 2013). Afterward, PLA_2-IIE-like contigs were identified, and their expression values were added to obtain an approximate value for PLA_2-IIE participation in each individual transcriptome. To better understand the phylogenetic history of the

PLA$_2$-IIE gene, we used the annotated PLA$_2$-IIE sequences from our sampled individuals and combined them with the PLA$_2$s from other publicly available vertebrates. The final nucleotide dataset was then aligned through its corresponding translated amino acid sequences using the MUSCLE algorithm (Edgar 2004), with 20 iterations and default parameters in Geneious v.2020.0.5 software. Phylogenetic tree inference was then carried out using IQ-Tree2 (Minh et al. 2020) by combining the substitution model estimation with ModelFinder, a tree search with 1000 replicates of ultrafast bootstrap and implementing the Shimodaira–Hasegawa approximate likelihood ratio test (SH-aLRT) and following the command recommended by the software developers. Moreover, we performed three additional tree searches using ultrafast bootstrap with 5000 replicates, a non-parametric bootstrap with 1000 replicates, both implemented in IQ-Tree2 (Minh et al. 2020) and a Bayesian approach in Mr. Bayes (Ronquist et al. 2012) using the nexus block available in the supplementary methods, Supplementary Material Online. Trees were visualized and edited using the iTol online platform (Letunic and Bork 2016). Orthology analyses were carried out for PLA$_2$-IIE transcripts recovered from the tribe with OrthoFinder v2.4.0 to identify possible duplication events within the tribe (Emms and Kelly 2019). An inflation parameter of 0.5 was used.

Enzymatic assay for PLA$_2$ activity.

Venom PLA$_2$ activities were assayed in 96-well plates using 4-nitro-3-(octanoyloxy) benzoic acid (NOB) as substrate in 0.1 M Tris-HCl, pH 8, containing 0.01 M Ca2+ as reaction buffer for 30 min at 37°C. The standard assay mixture contained 200 µl of buffer, 20 µl of substrate and 20 µl of venom (1 µg/µl) in a final volume of 240 µl. After adding the venom, reactions were run in a SpectraMax 340 plate reader for

30 min at 37°C, with the absorbance changes read at 425 nm. Venom from nine species of Pseudoboini were tested. Crude venoms from the viper *Bothrops jararacussu* and the CB subunit from the crotoxin of the rattlesnake, *Crotalus durissus*, were used as positive controls since they are recognized to have high PLA_2 activities (Freitas-De-sousa et al. 2020; Montoni et al. 2020). Venoms from colubrid snakes, *Philodryas olfersii* and *Thamnodynastes chaquensis*, were used as negative controls, since the venoms of these genera were reported to have low or no PLA_2 activity (Diaz et al. 2004; Ching et al. 2006; Correia et al. 2010; Zelanis et al. 2010; Ching et al. 2012). The obtained absorbance values were plotted for each sample, and the standard errors of the mean (SEM) were calculated for samples for which we had enough venom to run duplicate tests. To determine if there were significant differences among the groups, the nonparametric Kruskal–Wallis test was used. Multiple comparisons between the different groups were made through the nonparametric Wilcoxon test. All statistical tests were performed using R software version 4.1.0. Groups were considered significantly different if they had a p value < 0.05.

Structural analysis of the PLA_2-IIE from Pseudoboini

To understand the structural differences between PLA_2-IIEs from Pseudoboini and other snakes and the venom PLA_2-IIA from vipers, we aligned the primary structures of the assembled PLA_2-IIE to PLA_2-IIA/IIE sequences from other publicly available snakes. We used the MUSCLE algorithm (Edgar 2004), with 20 iterations and default parameters in Geneious v.2020.0.5 software. Then, to see how those differences in primary structure might affect the 3D organization of each protein, we predicted the 3D structures of PLA_2-

IIE from Pseudoboini and other snake species using the RoseTTAFold method implemented in the Robetta protein structure prediction server (Hiranuma et al. 2021). Predicted protein structures were only considered for further analyses if they had a predicted local distance difference test (l-DDT) higher than 0.80. We downloaded the crystal structure of a catalytically active PLA_2-IIA from *B. jararacussu* (UniProt code 1ZL7) and aligned it against our predicted models using the Matchmaker function available on ChimeraX 1.3 software. A fraction parameter of 1 was used to prioritize secondary structure over residue composition. The root-mean-square deviations of atomic positions (RMSD) of each alignment was used to estimate how well each of the models adjusted to the IIA structure.

Phylotranscriptomic analyses

First, we checked for putative sample contamination by assembling the mitochondrial sequences from each sample using MITGARD (v1.2) (Nachtigall, Grazziotin, et al. 2021) with the *Imantodes cenchoa* mitochondrial genome as reference (GenBank accession number EU728586.1). MITGARD is a tool that recovers the mitochondrial genome from RNA-seq data by using a reference as bait to retrieve the mitochondrial reads and use it to assemble the mitogenome. We annotate the assembled mitogenomes using MitoZ (v2.4) (Meng et al. 2019). Then, we used the assembled and annotated mitochondrial sequences to compare with previously obtained mitochondrial sequences of Pseudoboini species to validate the species identity. We also used 15 annotated mitochondrial genes (i.e., two ribosomal and 13 protein-coding) to infer a phylogenetic tree for each gene separately. To do this, we aligned their sequences using MAFFT (v7.310) (Katoh and Standley 2014), trimmed the alignments using trimAl (v1.2)

(Capella-Gutiérrez et al. 2009) with the "-automated1" parameter, and built trees using IQ-TREE (v2.0.3) (Minh et al. 2020). Branches with Bootstrap values lower than or equal to 95 were removed from each mitochondrial gene tree using the newick utilities package (v1.6) (Junier and Zdobnov 2010) and the final consensus tree was generated using the coalescent approach implemented in Astral (v5.15.4) (Mirarab et al. 2014).

Then, we employed the software BUSCO (v5.2.2) (Manni et al. 2021), which infers measurements of genome and transcriptome completeness based on evolutionary informed expectations of gene content through the use of sets of lineage-specific sets benchmarking universal single-copy orthologs. We used the "aves_odb10" set (total of 8338 genes in the BUSCO set) that represents the set with closer relationship to snakes among all other BUSCO sets and allowed the recovery of a higher number of nuclear loci to be used in the tree inference. We retrieved a total of 5359 loci and filtered it to only keep loci containing at least 15 samples to avoid bias related to missing data, which resulted in a final set containing 2161 loci. We aligned each locus separately in the final set using MAFFT (v7.310) (Katoh and Standley 2014) with the parameters "--auto" and "--adjustdirectionaccurately". The alignments were cleaned using CIAlign (v1.0.14) (Tumescheit et al. 2022), with the following parameters "--remove_divergent --remove_divergent_minperc 0.80 --remove_insertions --crop_ends --remove_short". The alignments were trimmed using trimAl (v1.2) (Capella-Gutiérrez et al. 2009) with the "-strictplus" parameter. The trimmed alignments were used to infer the phylogenetic trees for each locus using IQ-TREE (v2.0.3) (Minh et al. 2020). Then, branches with Bootstrap values lower than or equal to 95 were removed from each locus tree using the newick utilities package (v1.6) (Junier and Zdobnov 2010) and the final consensus tree was

generated using the coalescent approach implemented in Astral (v5.15.4) (Mirarab et al. 2014).

Data Availability

Raw transcriptomic data are available at NCBI's GenBank under Bioproject accession number PRJNA625548. Curated sequences (CDS) for all toxin transcripts generated in this work are available in the Supplementary Table S1, organized per species. Additional supplementary information (i.e., RAW proteomic data and multiple sequence alignments for phylogenetic analyses is available in a Figshare project (accessible at https://figshare.com/projects/Independent_recruitments_of_different_types_of_phospholipases_A2_to_the_venom_of_Caenophidian_snakes_the_rise_of_PLA2-IIE_within_Pseudoboini_Dipsadidae_/162772).

Supplementary Material

Supplementary data are available at Molecular Biology and Evolution online.

Acknowledgments

We thank Giuseppe Puorto (Reception of Venomous Animals of Instituto Butantan) and the team of students and technicians associated with the Laboratório de Coleções Zoológicas (LCZ - Instituto Butantan) and Facultad de Ciencias del Medio Ambiente (FACMA – Universidad Indoamérica) for the assistance in the field and in the processing of the biological material used in this study. We also thank Fiocruz's Technological

Platforms Network for using its proteomics core facility (Proteômica/RJ RPT2A Espectrometria de Massas), B.Sc. Joelma Saldanha for her technical assistance and Diego R. Quirola for his help in the field and in the laboratory. RHV is a fellow from Conselho Nacional de Desenvolvimento Científico e Tecnológico (CNPq), grant number 304523/ 2019-4. This work was also supported by grants from Fundação de Amparo à Pesquisa do Estado de São Paulo (2016/50127-5, 2013/07467-1, 2017/24498-9, and 2017/24546-3), and from Conselho Nacional de Desenvolvimento Científico e Tecnológico (309791/2017-0 and 303958/2018-9).

Figure Legends

Fig 1. Compositional profiles of venom-related transcripts in the Pseudoboini tribe. The phylogenetic tree was adapted from ZAHER et al., 2019 for general relationships outside of the tribe and was derived from our phylogenetic analyses for relationships within the tribe (Supplementary Fig. S1, Supplementary Material online). Bars represent the average amount of each annotated toxin type in the species. Pie plots to the right are from a representative species for each group. Note the elevated amount of PLA2 present in the Clelia-like group.

Fig. 2. (A) Multiple sequence alignment of PLA-IIEs from Pseudoboini and other snakes. Structural features are indicated by colored boxes. The aspartate residue, typical in catalytically active PLA2s, is highlighted in yellow. The asterisks indicate Pseudoboini PLA2-IIE with the C-terminal extension. The accession numbers for the

sequences from other snakes are gi_698375631, gi_384110785, XM_015820366, MN831292, XM_039367457, gi_1147529007, gi_25140376 and KX211996. (B) Protein sequence alignment of the highly and lowly expressed transcripts from representative species of the Clelia-like group. Dots indicate conserved amino acids between aligned sequences. Peptides identified by proteomic analyses are highlighted with red boxes. Heterogeneous regions found across the different proteins are indicated with light blue. The end of the signal peptide is marked by a red cross above residue 24. Total spectrum counts, unique peptides and coverages of mature proteins are indicated for identified proteins.

Fig. 3. Three-dimensional alignments of a B. *jararacussu* PLA2-IIA with different PLA2 forms from vipers and colubrid species. The table below displays the RMSD scores for each pairwise alignment. Yellow tones indicate better (lower) scores.

Fig. 4. Phylogenetic reconstruction of the assembled PLA2-IIE from Pseudoboini with PLA2s from other snakes using 1000 ultrafast bootstrap replicates. Assembled PLA2s from Pseudoboini cluster within the IIE subgroup, which is the sister group of PLA2s-IIA from vipers. Black crosses within the Pseudoboini tribe indicate sequences without the C-terminal extension commonly seen in endogenous PLA2-IIEs from other snakes. A schematic representation of multiple sequence alignments of full transcripts of PLA2-IIEs across sampled species exhibiting the variation of the C-terminal arrangement is shown to the right. The C-terminal region of the coding sequence is highlighted in blue. The 3'UTR of the full transcript is highlighted in green.

Dispholidus typus (Colubridae), some *Oxyrhopus* and all species from the Clelia-like group present a deletion before the stop codon, as indicated by red crosses.

Fig. 5. PLA_2 enzymatic activities measured for Pseudoboini venoms. Each color represents a different group of samples. Asterisks indicate significant differences between groups. SEM is plotted for each bar.

Fig. 6. Hypothetical genomic expansion events within each PLA_2 type among different snake families. Each colored box represents a gene. Physiological copies are assumed to be present in all snake groups. The open box shown in the Clelia-like group indicates the uncertainty of the physiological PLA_2-IIE gene structure, as we could not find a transcript without the C-terminal deletion in the sampled species. Genomic data are needed to reveal the true arrangement of the PLA_2-IIE gene in that group.

References

Armugam A, Gong NL, Li XJ, Siew PY, Chai SC, Nair R, Jeyaseelan K. 2004. Group IB phospholipase A2 from Pseudonaja textilis. *Arch. Biochem. Biophys.* [Internet] 421:10–20. Available from: https://pubmed.ncbi.nlm.nih.gov/14678780/

Bankar KG, Todur VN, Shukla RN, Vasudevan M. 2015. Ameliorated de novo transcriptome assembly using Illumina paired end sequence data with Trinity Assembler. *Genomics Data* [Internet] 5:352–359. Available from: https://www.sciencedirect.com/science/article/pii/S2213596015001567

Barbo FE, Marques OA V., Sawaya RJ. 2011. Diversity, Natural History, and Distribution of Snakes in the Municipality of São Paulo. *South Am. J. Herpetol.* [Internet] 6:135–160. Available from: https://bioone.org/journals/south-american-journal-of-herpetology/volume-6/issue-3/057.006.0301/Diversity-Natural-History-and-Distribution-of-Snakes-in-the-Municipality/10.2994/057.006.0301.full

Barua A, Mikheyev AS. 2019. Many Options, Few Solutions: Over 60 My Snakes Converged on a Few Optimal Venom Formulations. *Mol. Biol. Evol.* [Internet] 36:1964–1974. Available from: https://academic.oup.com/mbe/article-abstract/36/9/1964/5492084

Bayona-Serrano JD, Viala VL, Rautsaw RM, Schramer TD, Barros-Carvalho GA, Nishiyama MY, Freitas-de-Sousa LA, Moura-da-Silva AM, Parkinson CL, Grazziotin FG, et al. 2020. Replacement and Parallel Simplification of Nonhomologous Proteinases Maintain Venom Phenotypes in Rear-Fanged Snakes. *Mol. Biol. Evol.* [Internet] 37:3563–3575. Available from: https://academic.oup.com/mbe/article/37/12/3563/5877437

Bushmanova E, Antipov D, Lapidus A, Prjibelski AD. 2019. RnaSPAdes: A de novo transcriptome assembler and its application to RNA-Seq data. *Gigascience* [Internet] 8.

Available from: https://academic.oup.com/gigascience/article-abstract/8/9/giz100/5559527

Campos PF, Andrade-Silva D, Zelanis A, Leme AFP, Rocha MMT, Menezes MC, Serrano SMT, Junqueira-De-Azevedo IDLM. 2016. Trends in the evolution of snake toxins underscored by an integrative omics approach to profile the venom of the colubrid phalotris mertensi. *Genome Biol. Evol.* [Internet] 8:2266–2287. Available from: https://academic.oup.com/gbe/article-abstract/8/8/2266/2198055

Capella-Gutiérrez S, Silla-Martínez JM, Gabaldón T. 2009. trimAl: a tool for automated alignment trimming in large-scale phylogenetic analyses. *Bioinformatics* [Internet] 25:1972–1973. Available from: https://academic.oup.com/bioinformatics/article/25/15/1972/213148

Chang Z, Li G, Liu J, Zhang Y, Ashby C, Liu D, Cramer CL, Huang X. 2015. Bridger: A new framework for de novo transcriptome assembly using RNA-seq data. *Genome Biol.* 16.

Ching ATC, Paes Leme AF, Zelanis A, Rocha MMT, Furtado MDFD, Silva DA, Trugilho MRO, Da Rocha SLG, Perales J, Ho PL, et al. 2012. Venomics profiling of Thamnodynastes strigatus unveils matrix metalloproteinases and other novel proteins recruited to the toxin arsenal of rear-fanged snakes. *J. Proteome Res.* 11:1152–1162.

Ching ATC, Rocha MMT, Paes Leme AF, Pimenta DC, de Fátima D. Furtado M, Serrano SMT, Ho PL, Junqueira-de-Azevedo ILM. 2006. Some aspects of the venom proteome of the Colubridae snake Philodryas olfersii revealed from a Duvernoy's (venom) gland transcriptome. *FEBS Lett.* 580:4417–4422.

Chippaux JP. 2015. Epidemiology of envenomations by terrestrial venomous animals in Brazil based on case reporting: From obvious facts to contingencies. *J. Venom. Anim. Toxins Incl. Trop. Dis.* [Internet] 21:1–17. Available from: http://www.scielo.br/j/jvatitd/a/r9ZgKxxmd5xvjqd4WD8g3Kv/abstract/?lang=en

Chomzynski P. 1987. Single-Step Method of RNA Isolation by Acid Guanidinium Thiocyanate–

Phenol–Chloroform Extraction. *Anal. Biochem*. 162:156–159.

Correia JM, Santana Neto P de L, Pinho MSS, Silva JA da, Amorim MLP, Escobar JAC. 2010. Poisoning due to Philodryas olfersii (Lichtenstein, 1823) attended at Restauração Hospital in Recife, State of Pernambuco, Brazil: case report. *Rev. Soc. Bras. Med. Trop.* [Internet] 43:336–338. Available from: http://www.scielo.br/scielo.php?pid=S0037-86822010000300025&script=sci_arttext

Diaz F, Navarrete LF, Pefaur J, Rodriguez-Acosta A. 2004. Envenomation by neotropical opistoglyphous colubrid Thamnodynastes cf. pallidus Linné, 1758 (serpentes:colubridae) in Venezuela. *Rev. Inst. Med. Trop. Sao Paulo* 46:287–290.

Dowell NL, Giorgianni MW, Kassner VA, Selegue JE, Sanchez EE, Carroll SB. 2016. The Deep Origin and Recent Loss of Venom Toxin Genes in Rattlesnakes. *Curr. Biol.* [Internet] 26:2434–2445. Available from: http://dx.doi.org/10.1016/j.cub.2016.07.038

Edgar RC. 2004. MUSCLE: A multiple sequence alignment method with reduced time and space complexity. *BMC Bioinformatics* 5.

Egozcue JJ, Pawlowsky-Glahn V, Mateu-Figueras G, Barceló-Vidal C. 2003. Isometric Logratio Transformations for Compositional Data Analysis. *Math. Geol.* [Internet] 35:279–300. Available from: https://link.springer.com/article/10.1023/A:1023818214614

Emms DM, Kelly S. 2019. OrthoFinder: Phylogenetic orthology inference for comparative genomics. *Genome Biol.* [Internet] 20:1–14. Available from: https://link.springer.com/articles/10.1186/s13059-019-1832-y

Filzmoser P, Hron K, Reimann C. 2009. Univariate statistical analysis of environmental (compositional) data: Problems and possibilities. *Sci. Total Environ.* 407:6100–6108.

Fox J, Serrano S. 2007. Approaching the Golden Age of Natural Product Pharmaceuticals from Venom Libraries: An Overview of Toxins and Toxin-Derivatives Currently Involved in

Therapeutic or Diagnostic Applications. *Curr. Pharm. Des.* 13:2927–2934.

Freitas-De-sousa LA, Nachtigall PG, Portes-Junior JA, Holding ML, Nystrom GS, Ellsworth SA, Guimarães NC, Tioyama E, Ortiz F, Silva BR, et al. 2020. Size Matters: An Evaluation of the Molecular Basis of Ontogenetic Modifications in the Composition of Bothrops jararacussu Snake Venom. *Toxins 2020, Vol. 12, Page 791* [Internet] 12:791. Available from: https://www.mdpi.com/2072-6651/12/12/791/htm

Fry B. 2015. Venomous reptiles and their toxins: evolution, pathophysiology, and biodiscovery. 1st ed. USA: Oxford Uiversity Press Available from: https://books.google.com.br/books?hl=pt-BR&lr=&id=mRHwBwAAQBAJ&oi=fnd&pg=PP1&dq=Fry,+B.+(Ed.).+(2015).+Venomous+reptiles+and+their+toxins:+evolution,+pathophysiology+and+biodiscovery.+Oxford+University+Press.&ots=vedMHBslMm&sig=ELmmOkBgxy17aqZ3inPNfx4H2X8

Fry BG, Scheib H, Junqueira de Azevedo I de LM, Silva DA, Casewell NR. 2012. Novel transcripts in the maxillary venom glands of advanced snakes. *Toxicon* 59:696–708.

Fry BG, Scheib H, van der Weerd L, Young B, McNaughtan J, Ramjan SFR, Vidal N, Poelmann RE, Norman JA. 2008. Evolution of an Arsenal. *Mol. Cell. Proteomics* [Internet] 7:215–246. Available from: http://www.mcponline.org/article/S1535947620312251/fulltext

Gaiarsa MP, Alencar LRV de, Martins M. 2013. Natural History of Pseudoboine Snakes. *Pap. Avulsos Zool.* [Internet] 53:261–283. Available from: http://www.scielo.br/j/paz/a/bQbCFxVMb9gNTFcNyr8ghLK/?lang=en

Giraudo AR, Arzamendia V, Bellini GP, Bessa CA, Costanzo MB. 2014. Ecología de una gran serpiente Sudamericana, Hydrodynastes gigas (Serpentes: Dipsadidae). *Rev. Mex. Biodivers.* 85:1206–1216.

Grabherr MG, Haas BJ, Yassour M, Levin JZ, Thompson DA, Amit I, Adiconis X, Fan L,

Raychowdhury R, Zeng Q, et al. 2011. Full-length transcriptome assembly from RNA-Seq data without a reference genome. *Nat. Biotechnol.* 29:644–652.

Gutiérrez JM, Rucavado A, Chaves F, Díaz C, Escalante T. 2009. Experimental pathology of local tissue damage induced by Bothrops asper snake venom. *Toxicon* [Internet] 54:958–975. Available from: https://www.sciencedirect.com/science/article/pii/S0041010109001627?casa_token=pS8Z0afWa68AAAAA:7E_jftlfm6iP45T65-P-6Eu_7oX3Ft8TZ7gDTK1lawBVqUGWu5FtbuZi2G4CaUhbM-YmuhASK-ZR

Henderson RW. 1982. Trophic Relationships and Foraging Strategies of some New World Tree Snakes (Leptophis, Oxybelis, Uromacer). *Amphib. Reptil.* [Internet] 3:71–80. Available from: https://brill.com/view/journals/amre/3/1/article-p71_7.xml

Hiranuma N, Park H, Baek M, Anishchenko I, Dauparas J, Baker D. 2021. Improved protein structure refinement guided by deep learning based accuracy estimation. *Nat. Commun.* [Internet] 12:2020.07.17.209643. Available from: https://www.biorxiv.org/content/10.1101/2020.07.17.209643v2

Hofmann EP, Rautsaw RM, Strickland JL, Holding ML, Hogan MP, Mason AJ, Rokyta DR, Parkinson CL. 2018. Comparative venom-gland transcriptomics and venom proteomics of four Sidewinder Rattlesnake (Crotalus cerastes) lineages reveal little differential expression despite individual variation. *Sci. Rep.* [Internet] 8. Available from: https://www.nature.com/articles/s41598-018-33943-5

Holding ML, Margres MJ, Mason AJ, Parkinson CL, Rokyta DR. 2018. Evaluating the Performance of De Novo Assembly Methods for Venom-Gland Transcriptomics. *Toxins 2018, Vol. 10, Page 249* [Internet] 10:249. Available from: https://www.mdpi.com/2072-6651/10/6/249/htm

Huang P, Mackessy SP. 2004. Biochemical characterization of phospholipase A2 (trimorphin) from the venom of the Sonoran Lyre Snake Trimorphodon biscutatus lambda (family Colubridae). *Toxicon* 44:27–36.

Huang Q, Wu Y, Qin C, He W, Wei X. 2015a. Phylogenetic and structural analysis of the phospholipase A2 gene family in vertebrates. *Int. J. Mol. Med.* [Internet] 35:587–596. Available from: /pmc/articles/PMC4314415/

Huang Q, Wu Y, Qin C, He W, Wei X. 2015b. Phylogenetic and structural analysis of the phospholipase A2 gene family in vertebrates. *Int. J. Mol. Med.* [Internet] 35:587–596. Available from: http://www.spandidos-publications.com/10.3892/ijmm.2014.2047/abstract

J. A, Ohno S. 1971. Evolution by Gene Duplication. *Popul. (French Ed.* [Internet] 26:1176. Available from: https://books.google.com.br/books?hl=es&lr=&id=5SjqCAAAQBAJ&oi=fnd&pg=PA1&dq=gene+duplication&ots=MnT6sGH-Ba&sig=VkR7yUh8xZWIGkiUOnnelZue3Q4&redir_esc=y#v=onepage&q=gene duplication&f=false

Jeyaseelan K, Armugam A, Donghui M, Tan NH. 2000. Structure and phylogeny of the venom group I phospholipase A2 gene. *Mol. Biol. Evol.* [Internet] 17:1010–1021. Available from: https://academic.oup.com/mbe/article/17/7/1010/1064668

Junier T, Zdobnov EM. 2010. The Newick utilities: high-throughput phylogenetic tree processing in the Unix shell. *Bioinformatics* [Internet] 26:1669–1670. Available from: https://academic.oup.com/bioinformatics/article/26/13/1669/200713

Junqueira-de-Azevedo ILM, Campos PF, Ching ATC, Mackessy SP. 2016. Colubrid Venom Composition: An -Omics Perspective. *Toxins (Basel).* [Internet] 8:1–24. Available from: http://www.mdpi.com/2072-6651/8/8/230

Katoh K, Standley DM. 2014. MAFFT: Iterative refinement and additional methods. *Methods Mol. Biol.* [Internet] 1079:131–146. Available from: https://link.springer.com/protocol/10.1007/978-1-62703-646-7_8

Kini RM, Doley R. 2010. Structure, function and evolution of three-finger toxins: Mini proteins with multiple targets. *Toxicon* 56:855–867.

Koludarov I, Jackson TN, Pozzi A, Mikheyev AS. 2019. Family saga: Reconstructing the evolutionary history of a functionally diverse gene family reveals complexity at the genetic origins of novelty. *bioRxiv* [Internet]:583344. Available from: https://www.biorxiv.org/content/10.1101/583344v3

Krueger F. 2015. Trim Galore!: A wrapper tool around Cutadapt and FastQC to consistently apply quality and adapter trimming to FastQ files. *Babraham Inst.* [Internet]:https://www.bioinformatics.babraham.ac.uk/projects. Available from: https://github.com/FelixKrueger/TrimGalore

Letunic I, Bork P. 2016. Interactive tree of life (iTOL) v3: an online tool for the display and annotation of phylogenetic and other trees. *Nucleic Acids Res.* [Internet] 44:W242–W245. Available from: https://academic.oup.com/bioinformatics/article-abstract/23/1/127/188940

Li B, Dewey CN. 2011. RSEM: Accurate transcript quantification from RNA-Seq data with or without a reference genome. *BMC Bioinformatics* 12.

Lomonte B, Rey-Suárez P, Fernández J, Sasa M, Pla D, Vargas N, Bénard-Valle M, Sanz L, Corrêa-Netto C, Núñez V, et al. 2016. Venoms of Micrurus coral snakes: Evolutionary trends in compositional patterns emerging from proteomic analyses. *Toxicon* [Internet] 122:7–25. Available from: https://www.sciencedirect.com/science/article/pii/S0041010116302719?casa_token=zhTJdmuHtt4AAAAA:ZoDMO33OEc_kl_GLb79EZ-

fb7Sf8xjSO6fp1ujwkyGt4iC3I34ElrQLbZ6HdvmpQ3qrWKTSyDEa7

Mackessy SP. 2021. Handbook of Venoms and Toxins of Reptiles. 1st ed. Boca Raton: CRC Press Available from: https://www.taylorfrancis.com/books/9780429186394

Mackessy SP, Bryan W, Smith CF, Lopez K, Fernández J, Bonilla F, Camacho E, Sasa M, Lomonte B. 2020. Venomics of the Central American Lyre Snake Trimorphodon quadruplex (Colubridae: Smith, 1941) from Costa Rica. *J. Proteomics* 220:103778.

Mackessy SP, Sixberry NM, Heyborne WH, Fritts T. 2006. Venom of the Brown Treesnake, Boiga irregularis: Ontogenetic shifts and taxa-specific toxicity. *Toxicon* 47:537–548.

Manni M, Berkeley MR, Seppey M, Zdobnov EM. 2021. BUSCO: Assessing Genomic Data Quality and Beyond. *Curr. Protoc.* [Internet] 1:e323. Available from: https://onlinelibrary.wiley.com/doi/full/10.1002/cpz1.323

Meng G, Li Y, Yang C, Liu S. 2019. MitoZ: a toolkit for animal mitochondrial genome assembly, annotation and visualization. *Nucleic Acids Res.* [Internet] 47:e63–e63. Available from: https://academic.oup.com/nar/article/47/11/e63/5377471

Minh BQ, Schmidt HA, Chernomor O, Schrempf D, Woodhams MD, Von Haeseler A, Lanfear R, Teeling E. 2020. IQ-TREE 2: New Models and Efficient Methods for Phylogenetic Inference in the Genomic Era. *Mol. Biol. Evol.* [Internet] 37:1530–1534. Available from: https://academic.oup.com/mbe/article/37/5/1530/5721363

Mirarab S, Reaz R, Bayzid MS, Zimmermann T, S. Swenson M, Warnow T. 2014. ASTRAL: genome-scale coalescent-based species tree estimation. *Bioinformatics* [Internet] 30:i541–i548. Available from: https://academic.oup.com/bioinformatics/article/30/17/i541/200803

Modahl CM, Frietze S, Mackessy SP. 2018. Transcriptome-facilitated proteomic characterization of rear-fanged snake venoms reveal abundant metalloproteinases with enhanced activity. *J. Proteomics* [Internet] 187:223–234. Available from:

http://www.ncbi.nlm.nih.gov/pubmed/30092380

Montoni F, Andreotti DZ, Eichler RA dos S, Santos W da S, Kisaki CY, Arcos SSS, Lima IF, Soares MAM, Nishiyama-Jr MY, Nava-Rodrigues D, et al. 2020. The impact of rattlesnake venom on mice cerebellum proteomics points to synaptic inhibition and tissue damage. *J. Proteomics* 221:103779.

Nachtigall PG, Grazziotin FG, Junqueira-De-Azevedo ILM. 2021. MITGARD: an automated pipeline for mitochondrial genome assembly in eukaryotic species using RNA-seq data. *Brief. Bioinform.* [Internet] 22. Available from: https://academic.oup.com/bib/article/22/5/bbaa429/6123950

Nachtigall PG, Kashiwabara AY, Durham AM. 2021. CodAn: Predictive models for precise identification of coding regions in eukaryotic transcripts. *Brief. Bioinform.* [Internet] 22:1–11. Available from: https://academic.oup.com/bib/article/22/3/bbaa045/5847603

Nachtigall PG, Rautsaw RM, Ellsworth SA, Mason AJ, Rokyta DR, Parkinson CL, Junqueira-De-Azevedo ILM. 2021. ToxCodAn: A new toxin annotator and guide to venom gland transcriptomics. *Brief. Bioinform.* [Internet] 22:1–16. Available from: https://academic.oup.com/bib/article/22/5/bbab095/6235957

Ogawa T, Chijiwa T, Oda-Ueda N, Ohno M. 2005. Molecular diversity and accelerated evolution of C-type lectin-like proteins from snake venom. *Toxicon* 45:1–14.

Ogawa T, Kitajima M, Nakashima K ichi, Sakaki Y, Ohno M. 1995. Molecular evolution of group II phospholipases A2. *J. Mol. Evol.* [Internet] 41:867–877. Available from: https://link.springer.com/article/10.1007/BF00173166

de Oliveira L, Jared C, da Costa Prudente AL, Zaher H, Antoniazzi MM. 2008. Oral glands in dipsadine "goo-eater" snakes: Morphology and histochemistry of the infralabial glands in Atractus reticulatus, Dipsas indica, and Sibynomorphus mikanii. *Toxicon* 51:898–913.

Otero-Patiño R. 2009. Epidemiological, clinical and therapeutic aspects of Bothrops asper bites. *Toxicon* 54:998–1011.

Pla D, Petras D, Saviola AJ, Modahl CM, Sanz L, Pérez A, Juárez E, Frietze S, Dorrestein PC, Mackessy SP, et al. 2018. Transcriptomics-guided bottom-up and top-down venomics of neonate and adult specimens of the arboreal rear-fanged Brown Treesnake, Boiga irregularis, from Guam. *J. Proteomics* 174:71–84.

Pla D, Sanz L, Whiteley G, Wagstaff SC, Harrison RA, Casewell NR, Calvete JJ. 2017. What killed Karl Patterson Schmidt? Combined venom gland transcriptomic, venomic and antivenomic analysis of the South African green tree snake (the boomslang), Dispholidus typus. *Biochim. Biophys. Acta - Gen. Subj.* 1861:814–823.

Prado-Franceschi J, Hyslop S. 2002a. South American colubrid envenomations. *J. Toxicol. - Toxin Rev.* 21:117–158.

Prado-Franceschi J, Hyslop S. 2002b. SOUTH AMERICAN COLUBRID ENVENOMATIONS. *http://dx.doi.org/10.1081/TXR-120004744* [Internet] 21:117–158. Available from: https://www.tandfonline.com/doi/abs/10.1081/TXR-120004744

Rokyta DR, Lemmon AR, Margres MJ, Aronow K. 2012. The venom-gland transcriptome of the eastern diamondback rattlesnake (Crotalus adamanteus). *BMC Genomics* 13.

Ronquist F, Teslenko M, Van Der Mark P, Ayres DL, Darling A, Höhna S, Larget B, Liu L, Suchard MA, Huelsenbeck JP. 2012. MrBayes 3.2: Efficient Bayesian Phylogenetic Inference and Model Choice Across a Large Model Space. *Syst. Biol.* [Internet] 61:539–542. Available from: https://academic.oup.com/sysbio/article/61/3/539/1674894

Sevilla-Sánchez MJ, Ayerbe-González S, Bolaños-Bolaños E. 2021. Aspectos biomédicos y epidemiológicos del accidente ofídico en el departamento del Cauca, Colombia, 2009-2018. *Biomédica* [Internet] 41:314–337. Available from:

https://revistabiomedica.org/index.php/biomedica/article/view/5853

Six DA, Dennis EA. 2000. The expanding superfamily of phospholipase A2 enzymes: classification and characterization. *Biochim. Biophys. Acta - Mol. Cell Biol. Lipids* 1488:1–19.

Suranse V, Jackson TNW, Sunagar K. 2022. Contextual Constraints: Dynamic Evolution of Snake Venom Phospholipase A2. *Toxins (Basel).* [Internet] 14:420. Available from: https://www.mdpi.com/2072-6651/14/6/420/htm

Suzuki N, Ishizaki J, Yokota Y, Higashino K, Ono T, Ikeda M, Fujii N, Kawamoto K, Hanasaki K. 2000. Structures, Enzymatic Properties, and Expression of Novel Human and Mouse Secretory Phospholipase A2s *. *J. Biol. Chem.* [Internet] 275:5785–5793. Available from: http://www.jbc.org/article/S0021925818306136/fulltext

Tadokoro T, Modahl CM, Maenaka K, Aoki-Shioi N. 2020. Cysteine-Rich Secretory Proteins (CRISPs) from Venomous Snakes: An Overview of the Functional Diversity in a Large and Underappreciated Superfamily. *Toxins 2020, Vol. 12, Page 175* [Internet] 12:175. Available from: https://www.mdpi.com/2072-6651/12/3/175/htm

Tasoulis T, Lee MSY, Ziajko M, Dunstan N, Sumner J, Isbister GK. 2020. Activity of two key toxin groups in Australian elapid venoms show a strong correlation to phylogeny but not to diet. *BMC Evol. Biol.* [Internet] 20:1–13. Available from: https://bmcecolevol.biomedcentral.com/articles/10.1186/s12862-020-1578-x

Team RC. 2015. R: A Language and Environment for Statistical Computing. Vienna, Austria: R Foundation for Statistical Computing; 2014. R Foundation for Statistical Computing. *R Found. Stat. Comput. Vienna, Austria.* [Internet]. Available from: https://ci.nii.ac.jp/naid/20001692429/

Templ M, Hron K, Filzmoser P. 2011. robCompositions: An R-package for Robust Statistical

Analysis of Compositional Data. In: Compositional Data Analysis: Theory and Applications. p. 341–355. Available from: https://onlinelibrary.wiley.com/doi/pdf/10.1002/9781119976462#page=354

Torres-Bonilla KA, Andrade-Silva D, Serrano SMT, Hyslop S. 2018. Biochemical characterization of venom from Pseudoboa neuwiedii (Neuwied's false boa; Xenodontinae; Pseudoboini). *Comp. Biochem. Physiol. Part - C Toxicol. Pharmacol.* [Internet] 213:27–38. Available from: https://doi.org/10.1016/j.cbpc.2018.06.003

Torres-Bonilla KA, Floriano RS, Schezaro-Ramos R, Rodrigues-Simioni L, da Cruz-Höfling MA. 2017. A survey on some biochemical and pharmacological activities of venom from two Colombian colubrid snakes, Erythrolamprus bizona (Double-banded coral snake mimic) and Pseudoboa neuwiedii (Neuwied's false boa). *Toxicon* 131:29–36.

True JR, Carroll SB. 2002. Gene Co-Option in Physiological and Morphological Evolution. *Annu. Rev. Cell Dev. Biol.* 18:53–80.

Tsai I-H. 2016. Snake Venom Phospholipase A2: Evolution and Diversity. In: Venom Genomics and Proteomics. Springer Netherlands. p. 291–306.

Tumescheit C, Firth AE, Brown K. 2022. CIAlign: A highly customisable command line tool to clean, interpret and visualise multiple sequence alignments. *PeerJ* [Internet] 10:e12983. Available from: https://peerj.com/articles/12983

Uetz P, Freed P, Hošek J. 2019. The Reptile Database. Available from: http://www.reptile-database.org/

Vonk FJ, Casewell NR, Henkel C V., Heimberg AM, Jansen HJ, McCleary RJR, Kerkkamp HME, Vos RA, Guerreiro I, Calvete JJ, et al. 2013. The king cobra genome reveals dynamic gene evolution and adaptation in the snake venom system. *Proc. Natl. Acad. Sci. U. S. A.* 110:20651–20656.

Wagner GP, Kin K, Lynch VJ. 2012. Measurement of mRNA abundance using RNA-seq data: RPKM measure is inconsistent among samples. *Theory Biosci.* 131:281–285.

Wagner GP, Kin K, Lynch VJ. 2013. A model based criterion for gene expression calls using RNA-seq data. *Theory Biosci.* 132:159–164.

Weinstein SA, Warrell DA, White J, Keyler DE. 2011. "Venomous? Bites from Non-Venomous Snakes: A Critical Analysis of Risk and Management of "Colubrid? Snake Bites (Livre numérique Google). :364. Available from: http://books.google.com/books?hl=fr&lr=&id=lB3FxFG5wrQC&pgis=1

Wickham H. 2016. Data Analysis. :189–201. Available from: https://link.springer.com/chapter/10.1007/978-3-319-24277-4_9

Williams DJ, Faiz MA, Abela-Ridder B, Ainsworth S, Bulfone TC, Nickerson AD, Habib AG, Junghanss T, Fan HW, Turner M, et al. 2019. Strategy for a globally coordinated response to a priority neglected tropical disease: Snakebite envenoming. *PLoS Negl. Trop. Dis.* [Internet] 13:e0007059. Available from: https://journals.plos.org/plosntds/article?id=10.1371/journal.pntd.0007059

Yamaguchi K, Chijiwa T, Ikeda N, Shibata H, Fukumaki Y, Oda-Ueda N, Hattori S, Ohno M. 2014. The finding of a group IIE phospholipase A2 gene in a specified segment of Protobothrops flavoviridis genome and its possible evolutionary relationship to group IIA phospholipase A2 genes. *Toxins (Basel).* [Internet] 6:3471–3487. Available from: https://www.mdpi.com/2072-6651/6/12/3471/htm

Zaher H, Murphy RW, Arredondo JC, Graboski R, Machado-Filho PR, Mahlow K, Montingelli GG, Quadros AB, Orlov NL, Wilkinson M, et al. 2019. Large-scale molecular phylogeny, morphology, divergence-time estimation, and the fossil record of advanced caenophidian snakes (Squamata: Serpentes).

Zelanis A, Teixeira da Rocha MM, de Fátima Domingues Furtado M. 2010. Preliminary biochemical characterization of the venoms of five Colubridae species from Brazil. *Toxicon* 55:666–669.

Zhang J, Kobert K, Flouri T, Stamatakis A. 2014. PEAR: A fast and accurate Illumina Paired-End reAd mergeR. *Bioinformatics* [Internet] 30:614–620. Available from: https://academic.oup.com/bioinformatics/article-abstract/30/5/614/247231

Zhang Y. 2015. Why do we study animal toxins? *Zool. Res.* [Internet] 36:183. Available from: /pmc/articles/PMC4790257/

Zybailov B, Mosley AL, Sardiu ME, Coleman MK, Florens L, Washburn MP. 2006. Statistical analysis of membrane proteome expression changes in Saccharomyces cerevisiae. *J. Proteome Res.* [Internet] 5:2339–2347. Available from: https://pubs.acs.org/doi/full/10.1021/pr060161n

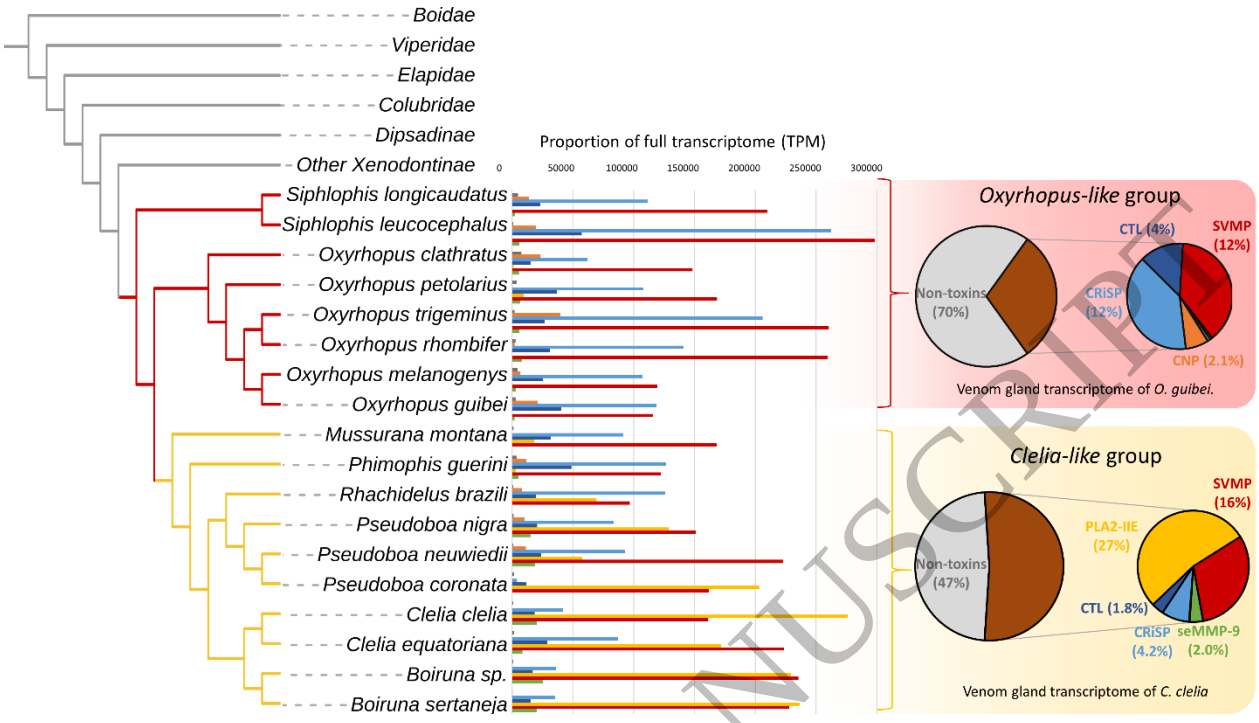

Figure 1
339x190 mm (x DPI)

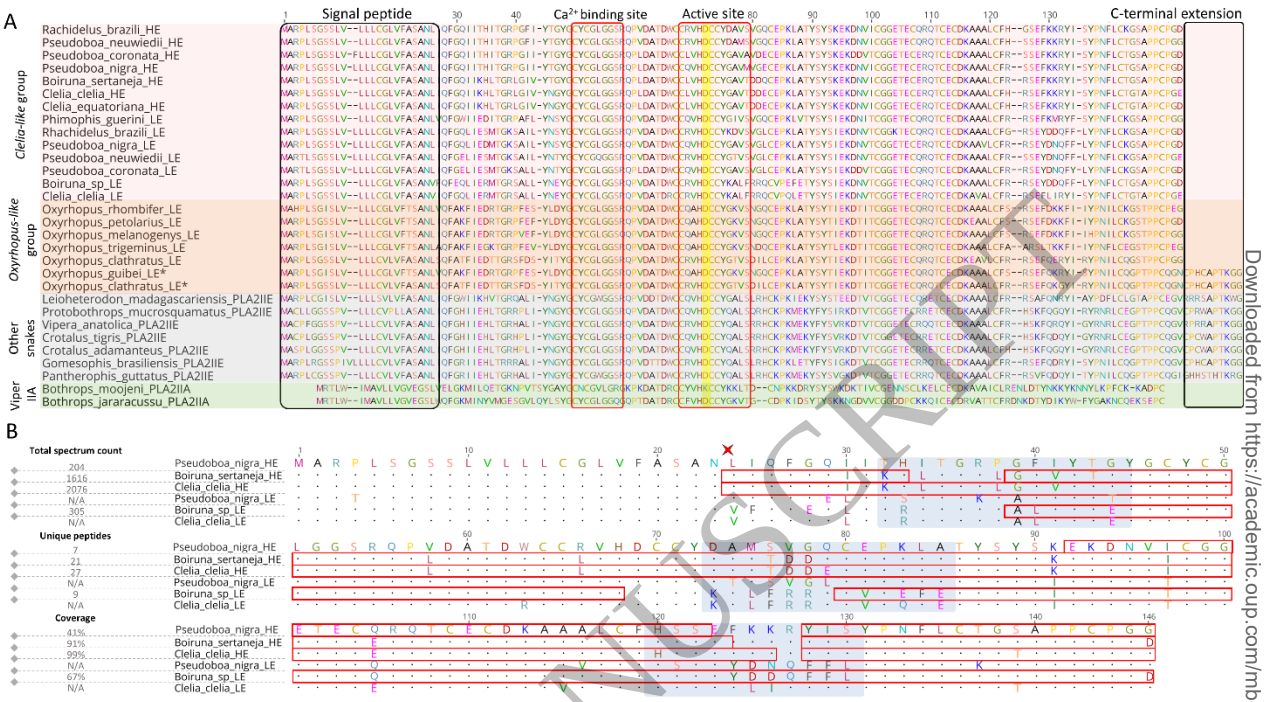

Figure 2
339x190 mm (x DPI)

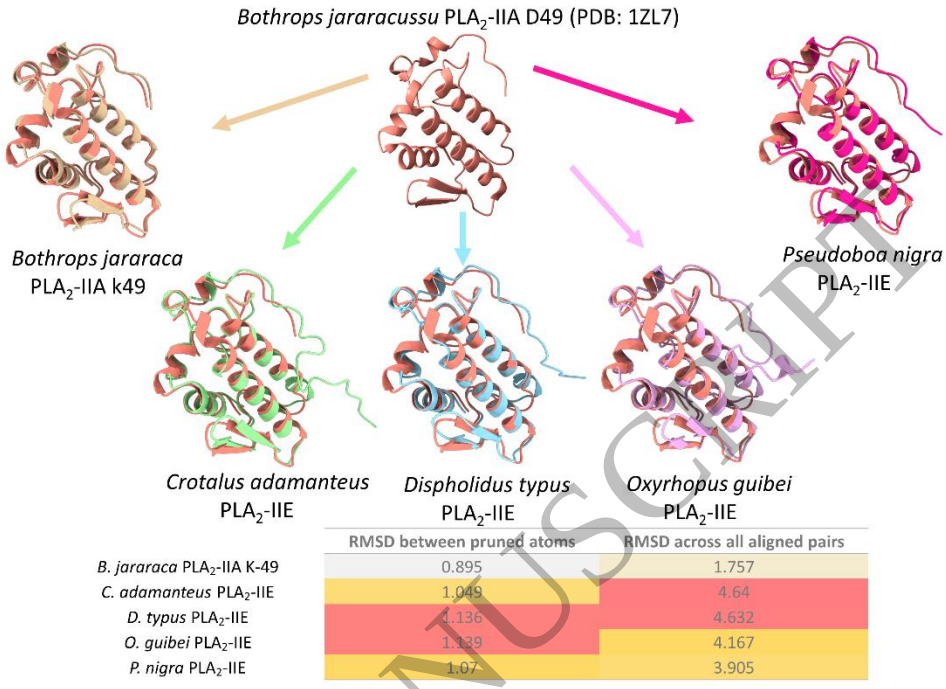

	RMSD between pruned atoms	RMSD across all aligned pairs
B. jararaca PLA$_2$-IIA K-49	0.895	1.757
C. adamanteus PLA$_2$-IIE	1.049	4.64
D. typus PLA$_2$-IIE	1.136	4.632
O. guibei PLA$_2$-IIE	1.139	4.167
P. nigra PLA$_2$-IIE	1.07	3.905

Figure 3
339x190 mm (x DPI)

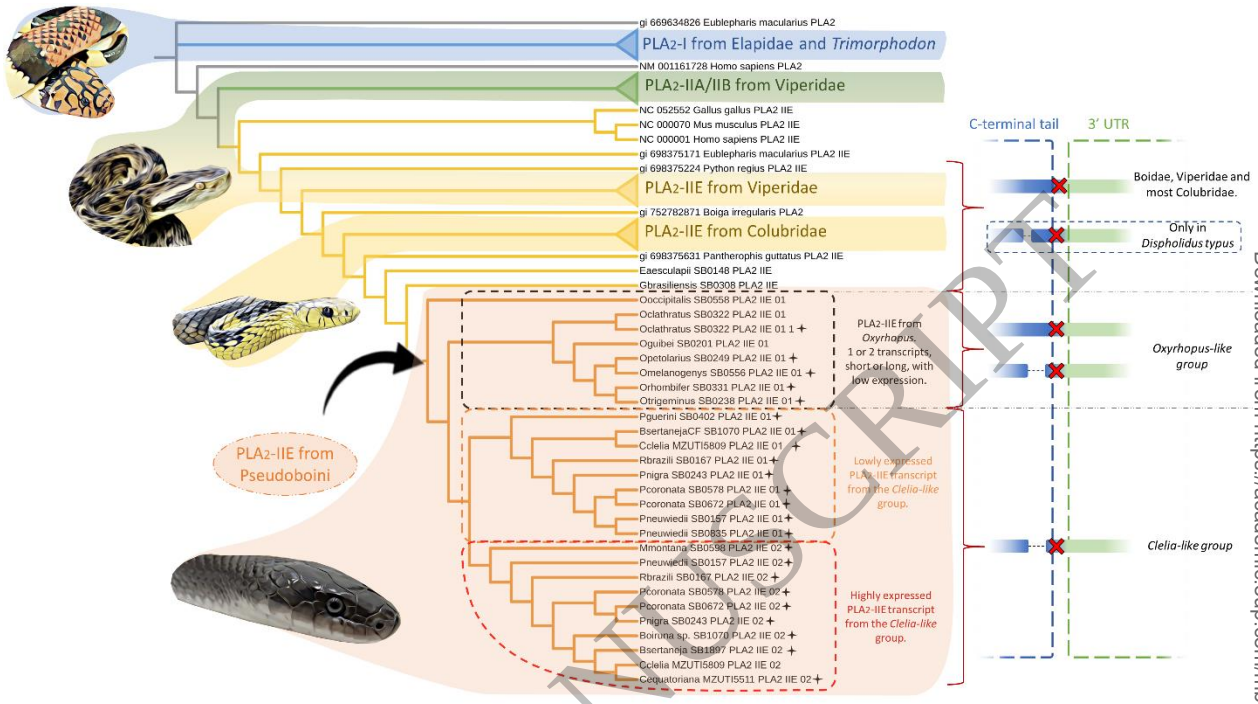

Figure 4
339x190 mm (x DPI)

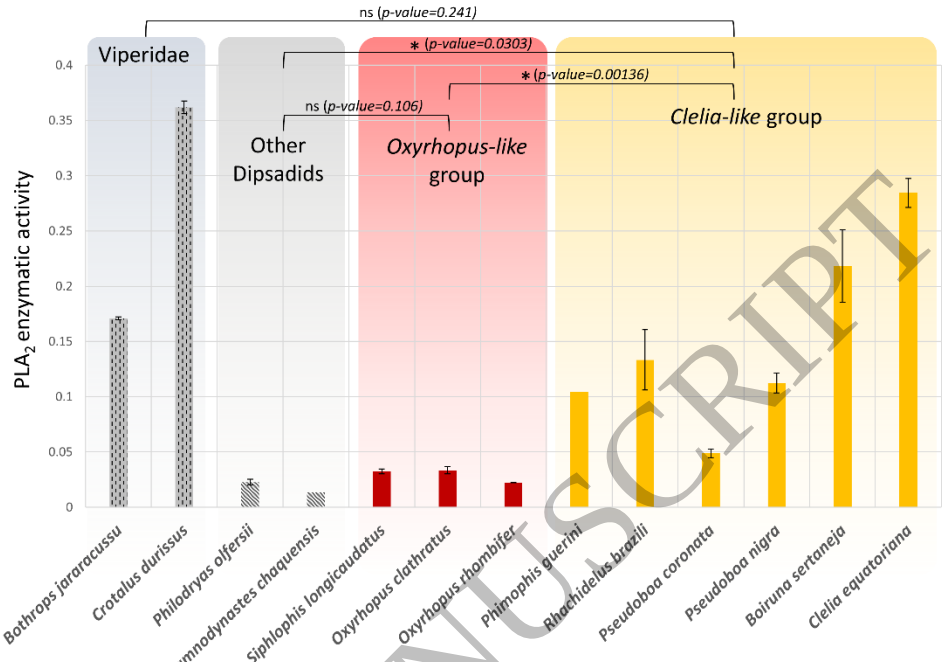

Figure 5
339x190 mm (x DPI)

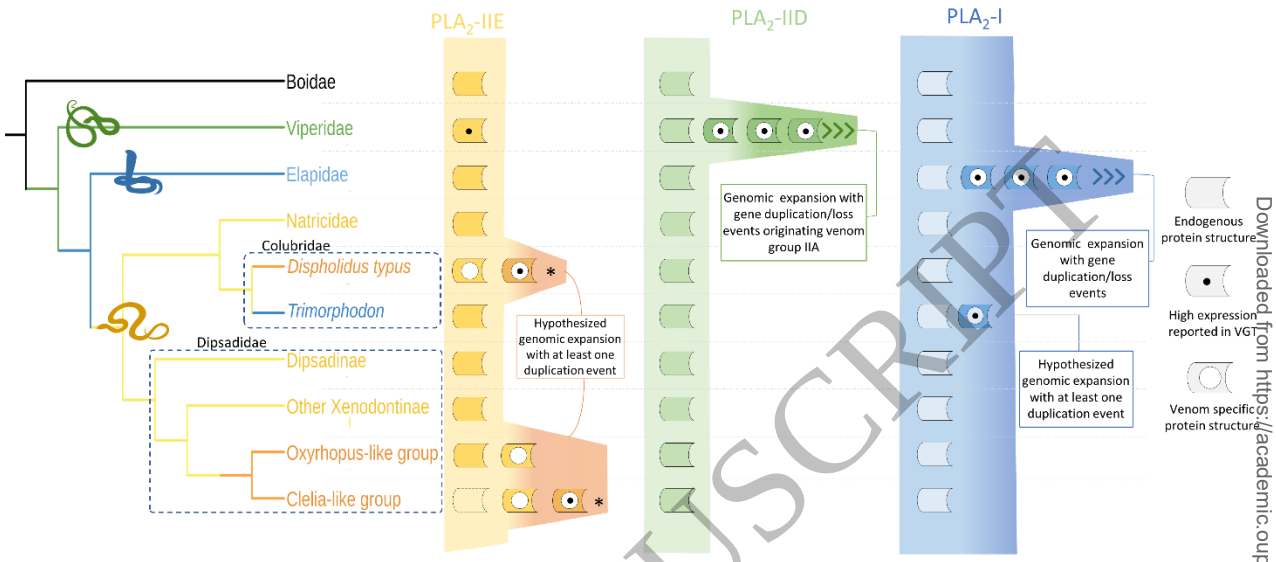

Figure 6
339x190 mm (x DPI)